

Band Pass Filter for Wideband Radar and EW Applications

Somsing Rathod^{1*}, Atul Kumar², K S Beenamol¹ and K P Ray²

¹Electronics and Radar Development Establishment, Defence Research and Development Organisation, Bengaluru, India

²Department of Electronics Engineering, Defence Institute of Advanced Technology, Girinagar, Pune, India

*Corresponding author E-mail:somsing.rathod@lrde.drdo.in

Abstract

The proposed design of wideband Band Pass Filter (BPF) utilizes composite filter design technique. This filter is used to achieve 3-dB bandwidth of 1-6GHz with more than 140% of Fractional Bandwidth (FBW). The fundamental design of composite BPF utilizes stepped impedance, Low Pass Filter (LPF) along with the quarter wavelength ($\lambda/4$) short circuited stubs. $\lambda/4$ short circuited stubs are incorporating High Pass Filter (HPF) response which transforms overall design into BPF. A modified design is developed with the help of a 3dB power divider and power coupler at input and output port respectively, to improve the roll-off at the lower cut-off frequency of the bandwidth. Both fundamental design and modified design are simulated and fabricated. Both simulated and measured results are presented, which are in agreement. This design is useful for wideband Radar and Electronic Warfare (EW) system.

Keywords: band pass filter, EW, radar receiver, wideband BPF, composite filter, receiver module.

1. Introduction

Ever increasing demand for higher bandwidth to provide better services for a large number of users with high data rates led to the development of wideband design technology[1]. In radar development, wideband technologies are required to develop EW applications and shared aperture techniques. Wideband Radars are also used in medical imaging applications such as Obstetrics imaging [2], Cardiology imaging (Radar stethoscope) [3] etc. The development of wideband component emerged with the advancement of wideband technologies [4]. Bandpass filters are one of the fundamental components required for the wideband designs like UWB receivers. The fractional bandwidth for a wideband BPF may vary from 50 to 100% or more. The conventional parallel coupled three-line microstrip structure in [5] has a fractional bandwidth of less than 70%. In [4], an alternate design utilizing a direct cascade of LPF and HPF to save circuit area and further optimizing it to make composite BPF has shown a significant improvement in fractional bandwidth with more than 100%.

This paper presents two different cases of BPF designs based on the composite BPF configuration of [4], with improved FBW and roll-off. In case-I, proposed BPF is developed with a size of 32.6mm X 7.0mm. In case-II, design with size 55.0mm X 18.0mm is developed with an improved roll-off when compared to case-I at the lower edge of the bandwidth (i.e. 1GHz). In order to minimize insertion loss (IL), both designs have been fabricated on RT/Duroid-5880. This substrate has very low loss tangent even at higher frequency upto 40GHz (i.e. $\tan\delta=0.0009$). Work carried out is oriented towards wideband radar and EW application.

2. Composite BPF Design and Calculation

The proposed composite BPF is developed using similar technique as in [4], stepped impedance LPF design along with the quarter

wavelength ($\lambda/4$) short circuited stubs at extremes of a stepped impedance LPF design, as shown in Fig.1. In this design, short circuited stubs incorporate HPF action along with the LPF for composing a BPF response. Short circuited stubs are separated so that overall structure emulate as BPF with pass band of 1 to 6GHz.

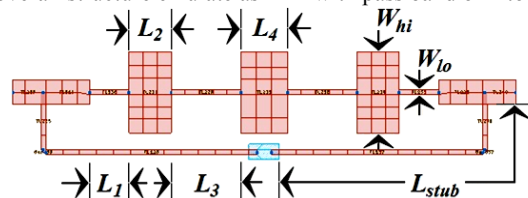


Fig.1. Layout of proposed BPF.

For stepped impedance LPF design, low-Z and high-Z values have been chosen, viz., 20Ω and 120Ω , respectively, for cut-off frequency (f) of 6GHz. The series inductor and shunt capacitor arrangement in conventional LPF design is replaced by high-Z and low-Z, respectively, in stepped impedance LPF design [6], as shown in Fig. (2).

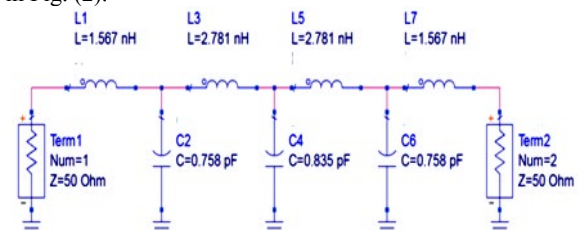


Fig.2 (a) Lumped Design using ADS

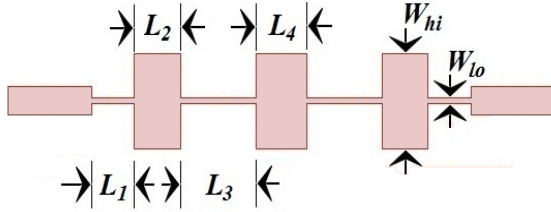


Fig.2 (b) Equivalent microstrip LPF

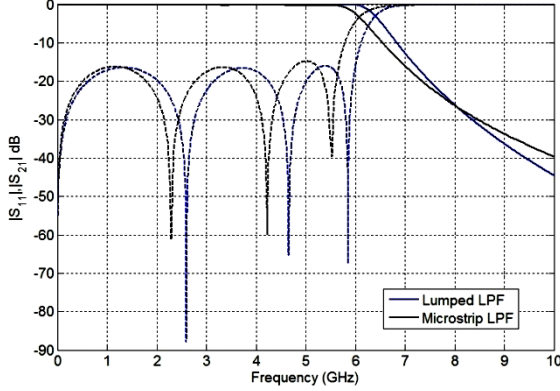


Fig.2 (c) Simulated Response

Fig.2 Conversion of lumped element design to microstrip layout of LPF for proposed BPF, (a) Lumped Design using ADS, (b) Equivalent microstrip LPF design with $L_1 = 2.55$, $L_2 = 2.73$, $L_3 = 4.52$, $L_4 = 3.02$, $W_{lo} = 5.22$, $W_{hi} = 0.30$, all in mm and (c) Simulated Response of lumped element design and its equivalent microstrip design.

The filter is designed with the Chebyshev prototype (the g_k) values for 0.1dB pass band ripple and 7th order of LPF are [6]: $g_1 = g_7 = 1.1812$, $g_2 = g_6 = 1.4288$, $g_3 = 2.0967$, $g_4 = g_5 = 1.5734$

Lumped components values for LPF designs are given in [6] as below:

Inductor:

$$L_k = \left(\frac{g_k}{2\pi f} \right) Z_0 \quad (1)$$

Capacitor:

$$C_k = \left(\frac{g_k}{2\pi f} \right) Z_0^{-1} \quad (2)$$

Component:

$$L_1 = L_7 = 1.567\text{nH}, C_2 = C_6 = 0.758\text{pF}, L_3 = L_5 = 2.781\text{nH}, C_4 = 0.835\text{pF}$$

Length of transmission lines [6]:

$$l_{inductor} = \frac{LZ_0}{Z_{hi}} \quad (3)$$

$$l_{capacitor} = \frac{CZ_{low}}{Z_0} \quad (4)$$

Where, L and C are the LPF prototypes (the g_k) values for a given pass band ripple and order of filter and Z_0 is the characteristic impedance of filter (i.e. 50 Ω).

Effective permittivity for high-Z ($\epsilon_{hi,eff}$) and low-Z ($\epsilon_{low,eff}$) lines are defined [7], as:

$$\epsilon_{eff} = \frac{\epsilon_r + 1}{2} + \frac{\epsilon_r - 1}{2} \left(1 + \frac{10H}{W} \right)^{-ab} \quad (5)$$

Where,

a =

$$1 + \frac{1}{49} \ln \left(\frac{\left(\frac{W}{H} \right)^4 + \left(\frac{W}{52H} \right)^2}{\left(\frac{W}{H} \right)^4 + 0.432} \right) + \frac{1}{18.7} \ln \left(\frac{\left(\frac{W}{H} \right)^4 + \left(\frac{W}{52H} \right)^2}{\left(\frac{W}{H} \right)^4 + 0.432} \right) \quad (5.a)$$

$$b = 0.564 \left(\frac{\epsilon_r - 0.9}{\epsilon_r + 3} \right)^{0.053} \quad (5.b)$$

W = Width of the transmission line
 Z_c = Characteristic Impedance of the transmission line

Width (W) and Characteristic Impedance (Z_c) for microstrip (stub and transmission) lines are related as [7]:

$$Z_c = \frac{\eta}{2\pi\sqrt{\epsilon_{eff}}} \ln \left(\frac{W}{H} F + \sqrt{\left(\frac{2H}{W} \right)^2 + 1} \right) \quad (6)$$

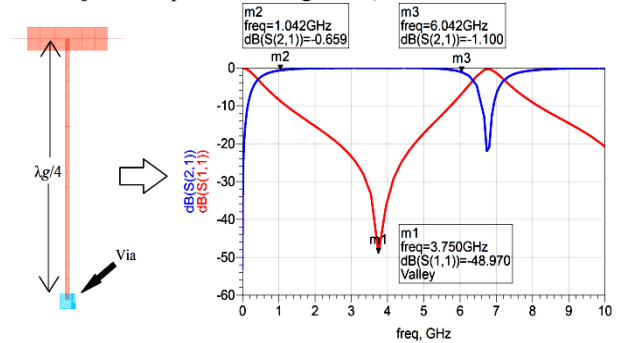
Where,

$$F = 6 + (2\pi - 6) \exp \left(-\frac{30.666H}{W} \right)^{0.7528} \quad (6.a)$$

Length of short circuited quarter wavelength stub of high-Z at center frequency (f_c) is:

$$L_{stub} = \frac{\lambda_0}{4\sqrt{\epsilon_{hi,eff}}} \quad (8)$$

Where, λ_0 is free space wavelength at f_c .

Fig.3 $\lambda_g/4$ short circuited stub layout and ADS Simulation Response.

As shown in Fig.3, Quarter wavelength stub indicates a flat S21 response for a wide range of frequency (~1 to 6GHz) and also it has a symmetric response about its resonating frequency (i.e. center frequency, $f_c = 3.5\text{GHz}$). Hence, this response is useful to make use of this stub along with LPF to form a BPF as in Fig.1.

Case-I: Fundamental Design

As shown in Fig. 4 (b), the measured response of this design matches well with the simulation response, which works for the frequency range of 1-6.5GHz. Length of the 50 ohm line is adjusted in such a manner, so that both the bent stubs share a common via, as shown in Fig.4 (a) and (c).

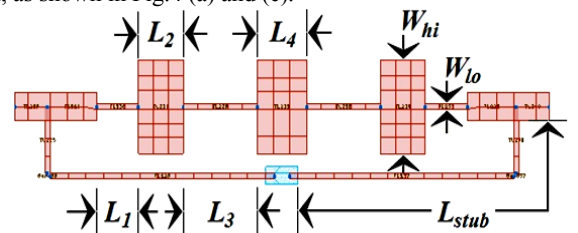


Fig.4 (a) Case-I: Equivalent microstrip LPF

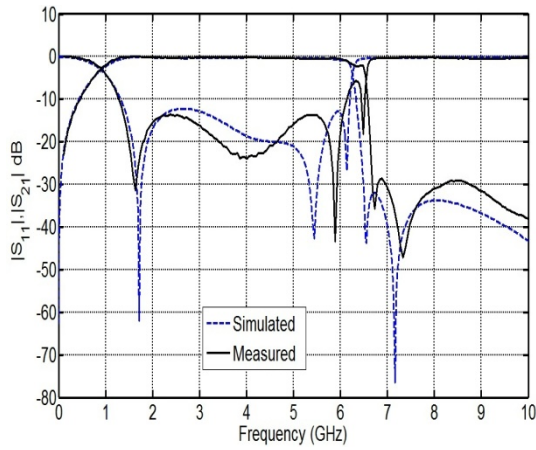


Fig. 4 (b) Case-I: Simulated and measured BPF performance

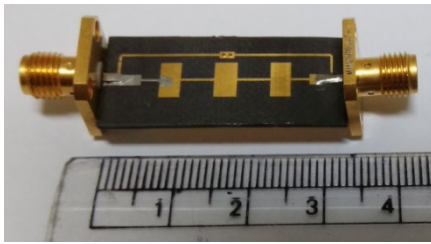


Fig. 4 (c) Case-I: Fabricated wideband BPF

Fig.4 (a) Geometry of the proposed BPF (Case-I). $L_1 = 2.55$, $L_2 = 2.73$, $L_3 = 4.52$, $L_4 = 3.02$, $W_{lo} = 5.22$, $W_{hi} = 0.29$, all in mm, circuit is symmetric about its centers. (b), Simulated and measured BPF performance. Both layout and simulation have been done by ADS-2016 and (c) Fabricated wideband BPF.

3. Analysis and Improvement

Filter response in case-I, clearly shows that near 1GHz roll-off is not sharp as it is near 6GHz. For getting a better rejection out of the band, sharp roll-off is essential at the edges. Making a parallel structure of two individual BPF of case-I will be most effective choice in order to increase the order of the filter for making an improvement in roll-off near 1GHz, rather than using a cascaded configuration. In a cascaded structure, overall insertion loss and input/output port reflection will be high, which degrades the performance of the filter.

3.1. Case-II: Modification to Improve the Roll-Off At Lower Edge of the Bandwidth

Two individual designs of case-I are combined with the help of power divider and power combiner at the input and output port, respectively to form a parallel combination of designs as shown in Fig.5. For this design, $S_{11} > -10$ dB and $S_{21} \sim -1.6$ dB in 5.5 to 6GHz. Therefore, the measured result degrades widely from simulation in this frequency range.

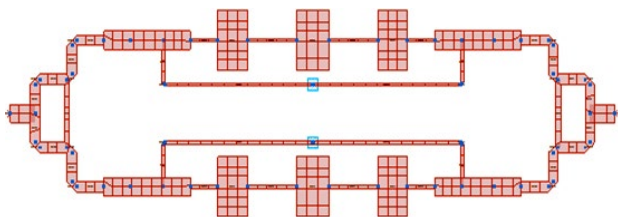


Fig.5 (a) Case-II: Modified filters structure for improved roll-off

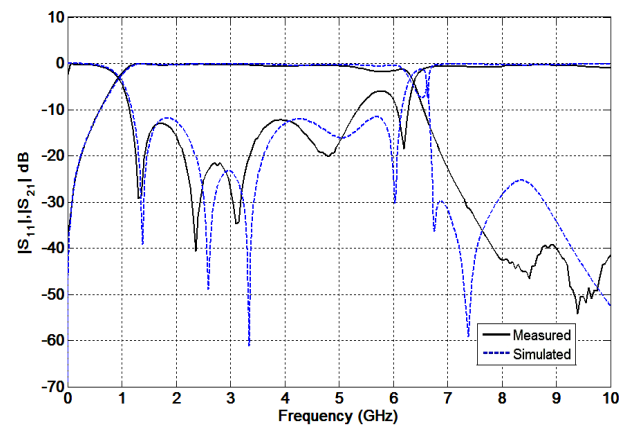


Fig.5 (b) Case-II: Simulated and measured BPF performance

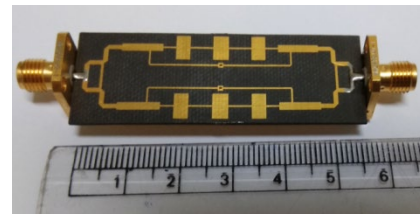


Fig.5 (c) Case-II: Fabricated wideband BPF

Table 1: Skirt details and Roll-off improvement

Parameters	Case-I	Case-II
S11 (Pass band)	-6.0 dB at 1.1GHz	-7.0 dB at 1.1GHz
	-21.0 dB at 3.5GHz	-21.0 dB at 3.5GHz
	-40.0 dB at 5.9GHz	-6.7 dB at 5.9GHz
S21 (Pass band)	-1.2 dB at 1.1GHz	-0.9 dB at 1.1GHz
	-0.11 dB at 3.5GHz	-0.5 dB at 3.5GHz
	-2.0 dB at 6.3GHz	-2.36 dB at 6.3GHz
S21 (Stop band)	-7 dB at 600MHz	-10 dB at 600MHz
	-10 dB at 450MHz	-13 dB at 450MHz
	-16 dB at 250MHz	-20 dB at 250MHz
	(lower edge skirt)	(lower edge skirt)
	-11 dB at 6.6GHz	-11 dB at 6.6GHz
	-30 dB at 7.0GHz	-23 dB at 7.0GHz
-38 dB at 10.0GHz	-38 dB at 10.0GHz	
(upper edge skirt)	(upper edge skirt)	
3-dB Bandwidth	0.9-6.5GHz	0.9-6.3GHz

4. Conclusion

A novel configuration of composite band pass filter has been presented with major emphasis on the enhancement of bandwidth and roll-off. In this manuscript all filters are designed for 1-6GHz with much improved FBW of about 140%, which is much higher than the value reported earlier. Use of this wideband filter, will lead to the development of Transmit/Receive Module (TRM) for the Active multipurpose Radars and Electronic Warfare systems.

Acknowledgement

We would like to thank Director Electronics and Radar Development Establishment (LRDE) and Mr. K Sreenivasulu, Divisional Officer, RAMD, LRDE Bengaluru. We would like to thank all LRDE colleagues for their unwavering support and motivation.

References

- [1] Y. Rahayu, T. A. Rahman, R. Ngah and P. S. Hall, "Ultra-wideband technology and its applications", 2008 5th IFIP International Conference on Wireless and Optical Communications Networks (WOCN '08), Surabaya, 2008, pp. 1-5
- [2] E. M. Staderini, "UWB Radars in medicine," in *IEEE Aerospace and Electronic Systems Magazine*, vol. 17, no. 1, pp. 13-18, Jan 2002. doi: 10.1109/62.978359

- [3] T. E. McEwan, "Body monitoring and imaging apparatus and method," *US Patent No.5,573,012*, Issued on November 12,1996
- [4] Ching-Luh Hsu, Fu-Chieh Hsu and J. K. Kuo, "Microstrip bandpass filters for Ultra-Wideband (UWB) wireless communications," *IEEE MTT-S International Microwave Symposium Digest*, 2005, pp. 4
- [5] J. T. Kuo and E. Shih, "Wideband bandpass filter design with three-line microstrip structures," in *IEE Proceedings - Microwaves, Antennas and Propagation*, vol. 149, no. 56, pp. 243-247, Oct/Dec 2002.
- [6] D. M. Pozar, *Microwave Engineering*, New York: *John Wiley & Sons*, 2nd Ed., 1998, ch. 8
- [7] Tzong-Lin Wu, "Microwave Filter Design", *Ch. 4. Transmission Lines and Components*.
<http://ntuenc.tw/upload/file/2011021716275842131.pdf>